



# INORGANIC CHEMISTRY

---

## FRONTIERS

## RESEARCH ARTICLE



Cite this: *Inorg. Chem. Front.*, 2016, 3, 397

Received 1st December 2015,  
Accepted 6th January 2016

DOI: 10.1039/c5qi00270b  
[rsc.li/frontiers-inorganic](http://rsc.li/frontiers-inorganic)

University of Zurich, Department of Chemistry, Winterthurerstrasse 190, 8057, Zurich, Switzerland. E-mail: [gilles.gasser@chem.uzh.ch](mailto:gilles.gasser@chem.uzh.ch); <http://www.gassergroup.com>;

Tel: +41 44 635 4630

† Electronic supplementary information (ESI) available. See DOI: 10.1039/c5qi00270b



Gilles Gasser

as Swiss National Science Foundation (SNSF) Ambizione fellow (2010) and then as a SNSF Assistant Professor (2011). Gilles is the recipient of several awards including the Werner Prize from the Swiss Chemical Society for outstanding independent chemical research (2015) and an ERC Consolidated Grant (2015).

## Insertion of organometallic moieties into peptides and peptide nucleic acids using alternative “click” strategies†

Cristina Mari, Sandro Mosberger, Nuria Llorente, Sarah Spreckelmeyer and Gilles Gasser\*

The insertion of metal complexes in biologically active systems is of great interest in view of diagnostic and therapeutic applications as well as a precious tool to unveil biological mechanisms. Optimization of safe and biocompatible reactions is critical to achieve high functionalization efficiency. Herein we present the application of two modified versions of copper-catalyzed azide–alkyne cycloaddition (*click*) chemistry, namely a one-pot diazotransfer + azide–alkyne cycloaddition (*one-pot click*) and a copper-free photoactivated tetrazole–alkene cycloaddition (*photoclick*), for derivatization of peptides and peptide nucleic acids (PNAs) with ferrocene and cymantrene moieties. These metal fragments were chosen for their possible exploitation as redox and IR probes. We could demonstrate that *one-pot click* enables for efficient functionalization of propargyl-glycine and an alkyne-containing peptide with an amino-containing cymantrene precursor. In addition, we could show that *photoclick* allows for the insertion of maleimido-ferrocene into a peptide and a PNA sequence containing a tetrazole moiety.

## Introduction

The functionalization of biologically active molecules is of great importance nowadays in medicinal chemistry.<sup>1–3</sup> In particular, their functionalization with metal-based compounds can confer novel properties to the formed bioconjugate compared to the biomolecule itself allowing for novel applications.<sup>4</sup> Metal complexes can be used as both diagnostic and therapeutic tools in the clinical treatment of patients.<sup>5</sup> The coupling of a targeting vector (*i.e.* peptide, antibody, *etc.*) to therapeutic/diagnostic metal-based drugs can, for example, increase their organ/cell selectivity.<sup>6–10</sup> In a similar vein, the insertion of metal fragments into biologically active molecules can yield biocompatible and extremely useful tools for biological investigations, such as luminescent probes.<sup>11</sup>

The application of copper-catalyzed azide–alkyne cycloaddition (CuAAC, commonly referred to as click chemistry) for bioconjugation has been extensively exploited due to the high versatility, selectivity and functional group tolerance of this synthetic technique.<sup>12</sup> A great number of probes, including metal-containing probes, were “clicked” to an important variety of biologically active compounds such as peptides, antibodies, peptide nucleic acids (PNAs) or polymers.<sup>13–17</sup> However, this reaction presents two important drawbacks from both a chemical as well as a biological point of view. Since an azide is one of the protagonists of this transformation, this functional group



has to be installed on one of the two molecules to be coupled. Safety concerns about the isolation of azides (especially with low molecular weight compounds) are still actual nowadays due to the potential instability of this class of compounds.<sup>18</sup> Therefore, from a chemical point of view, it would be more convenient to skip the azide isolation, for example, *via* an *in situ* insertion of this functionality. The second disadvantage of the CuAAC is its reliability on the presence of Cu<sup>I</sup> as catalyst for its mechanism to take place. This situation represents a problem for *in cellulo* applications of the technique due to the toxicity of the metal.<sup>13,19</sup> To address these limitations, a great effort has been made towards the optimization of new methodologies for click-mediated biocompatible conjugation.<sup>13,20,21</sup> Since the absence of a Cu catalyst makes the click reaction very inefficient, an alternative activation mechanisms had to be developed. Among the most relevant examples, Strain-Promoted Inverse Electron Demand Diels–Alder Cycloaddition (SPIEDAC) and Strain-Promoted Alkyne–Azide Cycloaddition (SPAAC) exploit the formation of an unstrained product as reaction driving force, circumventing the need of Cu catalysis.<sup>19</sup> Other approaches involve the use of light to form a reactive intermediate.<sup>21</sup>

Herein, we present, to the best of our knowledge, the first examples of the application of two modified versions of the classical CuAAC to introduce organometallic fragments into biologically active molecules, namely a peptide and a PNA oligomer (see Fig. 2). In particular, we focused our attention on two modified click reactions, namely the copper-catalyzed one-pot diazotransfer + azide–alkyne cycloaddition reaction (which will be called from now on in this article *one-pot click*)<sup>22</sup> and the metal-free photoactivated tetrazole–alkene cycloaddition (referred to from now on as *photoclick*).<sup>23</sup> The two organometallic components investigated in this study were a cymantrene derivative **A** and a ferrocene derivative **B** (Fig. 1),<sup>24,25</sup> chosen for their potential use as IR (**A**) and redox (**B**) probes in a biological environment.<sup>26,27</sup>

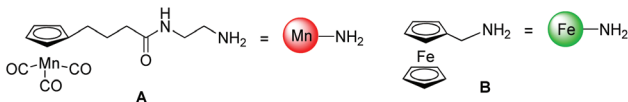


**Fig. 1** Structures of the organometallic complexes used in this paper and their simplified depictions.

## Results and discussion

### One-pot click reaction

The *one-pot click* reaction developed by Wittmann *et al.* allows in a subtle manner to circumvent the isolation of the azide intermediate.<sup>22</sup> More specifically, the *one-pot click* proceeds *via* two subsequent steps. First, an amine derivative is turned into an azide *via* a Cu<sup>II</sup> catalyzed diazotransfer. This intermediate can then be clicked to an alkyne by the classical CuAAC reaction. The Cu<sup>I</sup> catalyst for the click reaction is formed *in situ* by addition of a reducing agent to the mixture. In the present study, we applied this synthetic technique to the two amino-organometallic derivatives **A** and **B**. These molecules were clicked to an unnatural amino acid carrying a propargyl group (Fmoc-L-Pra-OH) and a short peptide containing this amino acid (**NLS-Pra**, Fig. 2). This small peptide is known for its nuclear targeting properties and has been used in the past by our group to deliver different metal complexes to the cell nucleus.<sup>6,28,29</sup> **NLS-Pra** was synthesized by standard solid phase synthesis and the alkynyl containing unnatural amino acid was inserted at the *N*-terminus.<sup>28</sup> The original *one-pot click* procedure reported by Wittmann *et al.* was followed in this study with the exception of minor modifications: the amounts of copper salt, tris(benzyltriazolylmethyl)amine (TBTA) and sodium ascorbate were doubled and the reaction duration was extended to 1 h of microwave assisted refluxing, instead of 30 minutes. When **A** was used as the amine precursor, the reaction was found to be effective for labelling both the amino acid and the peptide (Fig. 3).

More specifically, product **2A** was isolated in 50% yield and its structure confirmed by several analytical techniques. The UPLC-MS chromatogram showed one peak, whose integrated mass of *m/z* 694.2 is attributable to [M + H]<sup>+</sup>. The nature of **2A** was further confirmed by HR ESI-MS, in which the peak of [M – H]<sup>-</sup> is visible. In addition, the IR spectrum clearly showed the characteristic vibrations of the C=O groups at 1921 and 2015 cm<sup>-1</sup>. However, due to the presence of traces amounts of a paramagnetic impurity, we were unable to obtain a good <sup>1</sup>H-NMR spectrum. In the <sup>13</sup>C-NMR, however, resonances at 55.73 and 29.22 ppm can be attributed to the CH<sub>2</sub> and CH carbons between the newly formed triazole and the COOH moiety. The peptide derivative **3A** was isolated *via* preparative RP-HPLC purification. UPLC-MS analysis showed

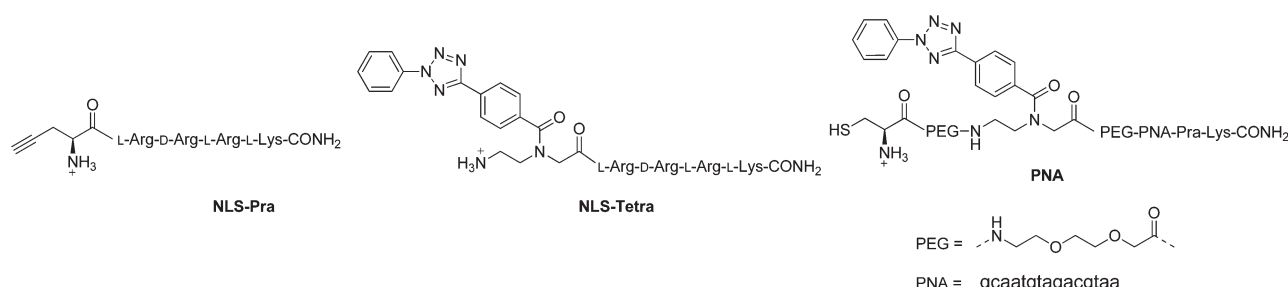


**Fig. 2** Structures of the peptides and PNA to be “clicked”. All amine groups in peptide and PNA sequences are present as TFA salts.



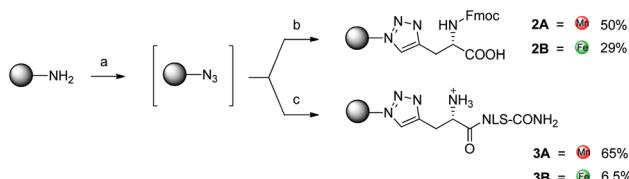


**Fig. 3** One-pot click reactions. (a)  $\text{TiN}_3$ ,  $\text{CuSO}_4$ ,  $\text{NaHCO}_3$ ,  $\text{H}_2\text{O}/\text{MeOH}/\text{DCM}$ , 30 min, RT. (b)  $\text{Fmoc-L-Pra-OH}$ , TBTA,  $\text{CuSO}_4$ , Na ascorbate, 1 h, MW 80 °C. (c)  $\text{NLS-Pra}$ , TBTA,  $\text{CuSO}_4$ , Na ascorbate, 1 h, MW 80 °C. All amine groups in the peptide sequence are present as TFA salts.

one peak in the chromatogram, with the  $m/z$  values assigned to the product with multiple charges. MALDI-TOF analysis also showed the expected peak at  $m/z$  1289.6 corresponding to  $[\text{M} + \text{H}]^+$ , but also the typical fragmentation of  $[\text{M} + \text{H} - \text{Mn}(\text{CO})_3]^+$ . Such a fragmentation was already reported for similar biomolecules.<sup>30</sup> As further confirmation of the identity of the compound, the IR spectrum of **3A** showed the vibrations of the  $\text{C}\equiv\text{O}$  at 1927 and 2017  $\text{cm}^{-1}$ . When the Fc precursor **B** was used as a reaction substrate, lower yields were observed for both the amino acid and the peptide labelling reactions. This is probably due to the instability of Fc-methylene compounds.<sup>31,32</sup> The harsh conditions of the click reaction (80 °C for 1 h) most probably led to partial decomposition of the ferrocene derivative. Nevertheless, products **2B** and **3B** could be isolated in 29% and 6.5% yields, respectively. For **2B**, the HR ESI-MS analysis showed the  $[\text{M} - \text{H}]^-$  peak at  $m/z$  575.1391 (calculated value: 575.1387). In addition, the  $^{13}\text{C}$ -NMR revealed the carbon signals of the newly formed triazole moiety at 144.70 and 124.25 ppm. Furthermore, 2D experiments correlated the resonance at 124.25 ppm to the broad peak at 7.77 ppm in the  $^1\text{H}$ -NMR, which could be then assigned to the triazole  $\text{CH}$ . For **3B**, MALDI-TOF analysis showed the most intense peak at  $m/z$  1172.6, which can be attributed to  $[\text{M} + \text{H}]^+$ .

### Photoclick reaction

As a parallel approach to the *one-pot click* reaction, we investigated the applicability of the *photoclick* reaction to our metal precursors, to pursue a more biocompatible method for organometallic labelling. This procedure exploits the light-mediated formation of a reactive acyl-nitrene intermediate from a tetrazole group. This activated intermediate is then prone to 1,3-dipolar cycloaddition with a substituted alkene.<sup>23</sup> This reaction belongs to the class of photo-mediated orthogonal reactions, which have been extensively exploited for *in vivo* applications due to their high selectivity and the lack of the toxic copper catalyst.<sup>20,21,33–35</sup> The diphenyltetrazole group **7**, which was synthesized as previously reported,<sup>36</sup> was installed on the PNA backbone **8**,<sup>37</sup> to obtain a tetrazole-containing PNA monomer as a *t*-Bu ester **9** (Fig. 4). Removal of the *t*-Bu yielded compound **10**, which can be inserted into a PNA or a peptide sequence by solid phase synthesis. The initial design of the system envisaged the use of a phenyl-allyloxy derivative as the

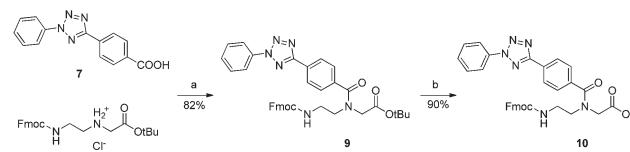


**Fig. 4** Synthesis of the tetrazole-containing PNA monomer. (a) HATU, HOEt, DIPEA, DMF, o.n., RT. (b) DCM : TFA : TIPS 2 : 1 : 0.4, o.n., RT.

alkene-reactive component. However, this molecule was found to be poorly reactive and only afforded the products in low yields. For these reasons, we decided to employ a maleimide group as alkene functionality. Maleimide derivatives of cymantrene and ferrocene (**4A** and **4B**, Fig. 5) were therefore prepared and “photoclicked” with the protected PNA monomer **9** bearing the tetrazole reactive moiety. The Fc-containing compound **5B** was isolated in 63% yield and fully characterized. The UV chromatogram of UPLC analysis showed one peak and the HR ESI-MS showed a peak at  $m/z$  912.3041, corresponding to  $[\text{M} + \text{H}]^+$  (calculated: 912.3054). On the other hand, the Mn derivative **5A** was isolated from the crude as a minor component (8.5%), whereas the main product of the reaction (40%) was still a product of *photoclick* lacking, however, the  $\text{Mn}(\text{CO})_3$  moiety ( $m/z$  891.5  $[\text{M} - \text{Mn}(\text{CO})_3 + \text{H}]^+$ ). Comparison of the IR spectra confirmed the absence of the  $\text{C}\equiv\text{O}$  vibrations in the spectrum of the product isolated in higher amount, signals which are well visible in the IR spectrum of **5A** (1927 and 2019  $\text{cm}^{-1}$ ). This outcome is probably due to the known ability of cymantrenyl compounds to release CO upon light irradiation.<sup>38</sup> Therefore, it is likely that the product of the *photoclick* decomposes during the reaction.

Motivated by the successful formation of **5B**, we attempted the insertion of ferrocene-maleimide in a NLS peptide carrying

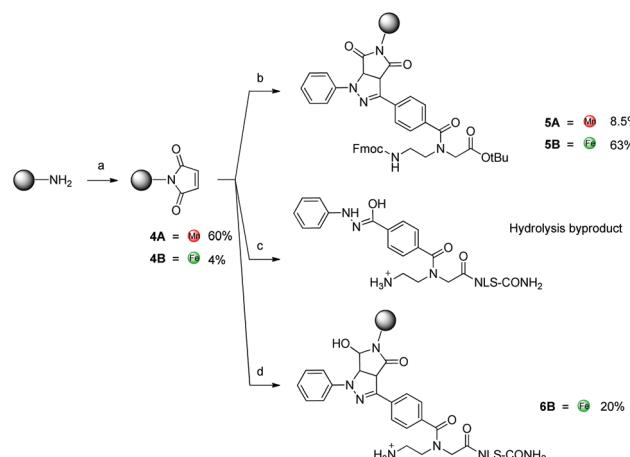


**Fig. 5** Photoclick reaction. (a) Maleic anhydride,  $\text{AcOH}$ , 8 h, reflux. (b) **9**,  $\text{ACN}$ , 302 nm, 1 h, RT. (c) **NLS-tetra**,  $\text{H}_2\text{O}$  or  $\text{ACN} : \text{PBS}$  (5 : 1), 302 nm, 30 min, RT. (d) **NLS-tetra**,  $\text{DMSO}$ , 302 nm, 1 h, RT. All amine groups in the peptide sequence are present as TFA salts.



the modified PNA monomer (**NLS-tetra**, Fig. 2), synthesized by solid phase synthesis.<sup>28</sup> In a procedure reporting on the modification of a DNA strand with a maleimide functionalized dye *via* photoclick, this reaction was performed in PBS affording yields in the range of 8–34% depending on the conditions used, whilst the use of DMSO as solvent did not afford the desired product.<sup>39</sup> Surprisingly, when we performed the reaction in water or ACN:PBS (5:1), after just 30 min irradiation **NLS-tetra** was found to have entirely turned into the hydrolysis byproduct of the acyl-nitrene intermediate (Fig. 5, ESI-MS (pos. detection mode):  $m/z$  [M + 3H]<sup>3+</sup> 318.4, [M + 2H]<sup>2+</sup> 476.9, [M + H]<sup>+</sup> 952.6. UPLC r.t. (2.5 min): 0.3 min). By performing the reaction in DMSO and upon 1 h irradiation, we could obtain, next to the hydrolysis compound, the expected product **6B** in 20% yield. MALDI-TOF analysis confirmed the identity of the compound, showing a peak at  $m/z$  1229.6 [M + H]<sup>+</sup>.

### PNA functionalization with photoclick

In order to assess the full potential of the *photoclick* synthetic procedure, we applied it to a PNA sequence. PNAs are DNA/RNA mimics which were first reported by Nielsen *et al.*<sup>40</sup> They have gained significant interest owing to their ability to hybridize with DNA/RNA complementary strands with very high affinity, their proven stability to nuclease and protease degradation and their lack of unspecific interactions with proteins. Thanks to these characteristics, PNAs are very promising for several applications ranging from nanotechnology<sup>41,42</sup> to *in vivo* antisense therapy<sup>43</sup> and tumour pre-targeting.<sup>8</sup> However, there is room for improvement of the potential of PNAs in biological applications, for example by increasing their low solubility in physiological environment or by equipping them with a probe for cellular localization. It is therefore important to develop techniques for PNA functionalization. In particular,

substitution with metal complexes have been of great interest to exploit additional properties of the new PNA–metal complex conjugate.<sup>8,15,16,37,44–51</sup> In this work, we applied *photoclick* to achieve the insertion of a ferrocene moiety into a PNA sequence that was previously applied as an antisense agent on hepatitis B virus.<sup>52</sup> This sequence, which was synthesized *via* solid phase synthesis,<sup>53</sup> was further modified with the insertion of the PNA monomer bearing the modified tetrazole and a cysteine for conjugation *via* Michael addition (**PNA**, Fig. 2). The *photoclick* reaction was performed several times to optimize the conditions and the structures of the isolated products are reported in Fig. 6. Having the PNA sequence as substrate, the reaction showed a similar behaviour to that reported previously with the DNA strand.<sup>39</sup> When DMSO was used as solvent, the **PNA** starting material was converted to the hydrolyzed form of the acyl-nitrene intermediate **14**. Therefore, in the second trial, the reaction was performed in water with 1 eq. of **4B**. After 1 h irradiation, we could isolate all the products reported in Fig. 6. The *photoclick* product **11**, containing a single Fc moiety, was isolated in 6.5% yield. The doubly Fc labelled PNA **12** was also formed in 8% yield, due to the occurrence of both *photoclick* and Michael addition. Furthermore **13**, a PNA containing the hydrolyzed tetrazole and the ferrocene conjugated at the cys group *via* Michael addition, was isolated in 14% yield. Due to the presence of water, the main component of the mixture was found to be the unlabelled hydrolyzed product **14** (30%). Next to these components, two compounds with  $m/z$  5380 and 5566, respectively were isolated but their structures were not elucidated. In the attempt to improve the labelling efficiency, increasing amounts of **4B** were used (5 eq.). The yield of formation of the *photoclick* product **11** could be increased to 10%. Additionally, the double Fc containing **12** was isolated in 2.6% yield, the hydrolyzed intermediate **14** in 17% yield and **13** in 36% yield. The

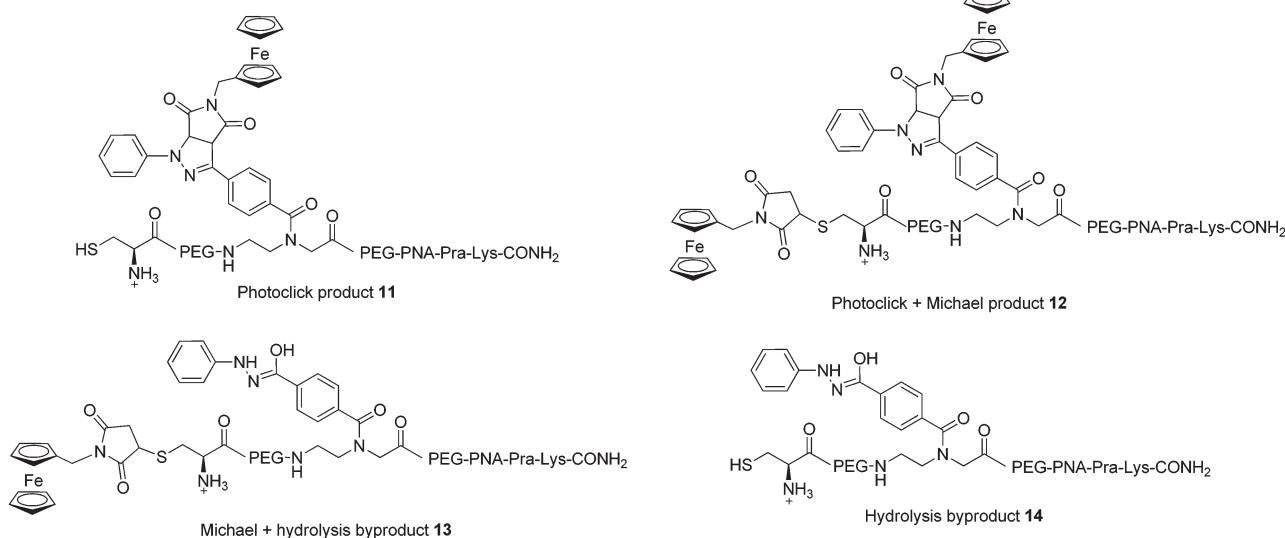


**Fig. 6** Products of the reaction between **PNA** and **4B** upon 302 nm light irradiation. All amine groups in the PNA sequences are present as TFA salts.



component with  $m/z$  5566 was also formed. As became evident from the last reaction conditions used, it is possible to increase the formation of the *photoclick* product by increasing the amount of the Fc-maleimide starting material. The kinetic of the competing Michael reaction seems however to be faster than the one of the *photoclick*, therefore, higher yields could be obtained if the cysteine would not be present.

## Experimental

### Instruments and methods

All commercial chemicals were used without further purification.  $^1\text{H}$  and  $^{13}\text{C}$  NMR measurements were carried out on Bruker 400 and 500 spectrometers and referenced to residual solvent peaks. The abbreviations for the peak multiplicities are as follows: s (singlet), bs (broad singlet), d (doublet), dd (doublet of doublets), t (triplet), q (quartet), m (multiplet). UV spectra were recorded on a Varian Cary 100 spectrophotometer. Elemental microanalyses were performed on a LecoCHNS-932 elemental analyser. ESI-MS and R.P. UPLC-MS were performed using a Bruker Daltonics HCT 6000 mass spectrometer. R.P. UPLC-MS spectra were recorded on a Waters Acquity<sup>TM</sup> system equipped with a PDA detector and an auto-sampler. R.P. UPLC-MS was performed on an Acquity UPLC BEH C18 column (21.50  $\times$  1.7 mm). The UPLC run (flow rate: 0.6 mL min $^{-1}$ ) was carried out with a linear gradient of A (double distilled water containing 0.1% v/v formic acid) and B (acetonitrile):  $t = 0$  min, 5% B;  $t = 0.25$  min, 5% B;  $t = 1.5$  min, 100% B;  $t = 2.5$  min, 100% B. High resolution ESI-MS spectra were recorded using a Bruker ESQUIRE-LC quadrupole ion trap instrument. The matrix-assisted laser desorption/ionization time of flight mass spectrometry (MALDI-TOF) mass spectra were measured on a Bruker Daltonics Autoflex. The experiments were performed in reflector (RP) or linear (LP) mode using  $\alpha$ -cyano-4-hydroxy-cinnamic acid on a Prespotted Anchor Chip (PAC HCCA) or sinapinic acid (SA) as the matrix. Preparative HPLC purification was carried out on a Varian ProStar system and an Agilent Zorbax 300 SB-C18 prep column (5  $\mu\text{m}$  particle size, 300  $\text{\AA}$  pore size, 150  $\times$  21.2 mm, flow rate: 20 mL min $^{-1}$ ). The runs were performed with a linear gradient of A (double distilled water containing 0.1% v/v trifluoroacetic acid) and B (acetonitrile, Sigma-Aldrich HPLC grade). Microwave reactions were performed using a Biotage Initiator + Robot Eight instrument in 2.5 mL sealed microwave vials. UV irradiation at 302 nm were performed using a handheld UV lamp UVM-57, 6 Watt from UVP, Cambridge, UK. Samples were irradiated in a Starna GmbH 1.4 or 3.5 mL fluorescence quartz cuvette (width 1 cm) while stirring.

### Syntheses

**A, B, 7, 8** were synthesized as previously described. All analytical data match with that reported in the literature.<sup>24,25,36,37</sup>

**Fmoc-PNA-tetra-OtBu 9.** The protected PNA backbone **8** as the chloride salt (517 mg, 1.195 mmol, 1.0 eq.) was dissolved in DCM (100 mL) and washed with  $\text{NaHCO}_3$  ( $2 \times 40$  mL). The

aqueous solution was back-extracted with DCM ( $2 \times 30$  mL). The organic phases were reunited and evaporated using a rotary evaporator to yield a yellow oil. **7** (350 mg, 1.31 mmol, 1.1 eq.) was dissolved in 10 mL of DMF. HATU (500 mg, 1.31 mmol, 1.1 eq.), HOEt (275 mg, 2.03 mmol, 1.7 eq.) and DIPEA (340  $\mu\text{L}$ , 2.03 mmol, 1.7 eq.) were then added to this solution and the mixture stirred for 20 min. The yellow oil containing **8** in 5 mL DMF was added to the mixture containing **7**. The mixture was stirred overnight. Afterwards, the solvent was removed at the rotary evaporator. The crude product was purified by column chromatography on silica gel with EtOAc : Hex (1 : 1) as the eluent to isolate the product (r.f. 0.65, 630 mg, 82%) as a yellowish solid. ESI-MS (pos. detection mode):  $m/z$  [M + Na] $^+$  667.2, [2M - H + Na] $^+$  1311.1.  $^1\text{H}$ -NMR  $\delta_{\text{H}}$  (CDCl<sub>3</sub>, 500 MHz): 1.44 (s, 9H, tBu), 3.29 (bs, 1H, NHCH<sub>2</sub>CH<sub>2</sub>), 3.54 (bs, 2H, NCH<sub>2</sub>CO), 3.75 (bs, 1H, NHCH<sub>2</sub>CH<sub>2</sub>), 3.93 (bs, 1H, CH<sub>2</sub>CH<sub>2</sub>N), 4.14 (bs, 1H, CH<sub>2</sub>CH<sub>2</sub>N), 4.24 (m, 1H, FMOC-CHCH<sub>2</sub>), 4.29–4.40 (dd, 2H, CHCH<sub>2</sub>O), 5.68 (bs, 1H, NH), 7.29–7.33 (t, 2H, FMOC), 7.38–7.42 (t, 2H, FMOC), 7.51–7.63 (m, 7H, FMOC + Ph), 7.77–7.79 (d, 2H, FMOC), 8.16–8.29 (m, 4H, Ph).  $^{13}\text{C}$ -NMR (CDCl<sub>3</sub>, 126 MHz, rotamers observed): 28.10, 39.34, 47.27, 47.35, 47.59, 49.14, 67.14, 120.04, 120.11, 125.26, 125.31, 127.21, 127.32, 127.46, 127.83, 129.86, 136.94, 141.43, 144.09, 156.29, 156.90, 164.52, 168.98, 169.23, 171.90, 172.64. HR ESI-MS calc for C<sub>37</sub>H<sub>37</sub>N<sub>6</sub>O<sub>5</sub> [M + H] $^+$  645.2028, found 645.2818, calc for C<sub>37</sub>H<sub>36</sub>N<sub>6</sub>O<sub>5</sub>Na [M + Na] $^+$  667.2639, found 667.2636.

**Fmoc-PNA-tetra-OH 10. 9** (350 mg, 0.54 mmol) was dissolved in 17 mL of a DCM : TFA : TIPS (2 : 1 : 0.4) solution. The mixture was stirred overnight at room temperature. The solvent was then removed at the rotary evaporator and the crude product purified by column chromatography on silica gel with eluent EtOAc : MeOH (10 : 3) to isolate the product as a white powder (r.f. 0.55, 320 mg, 90%). ESI-MS (pos. detection mode):  $m/z$  [M + H] $^+$  589.3, [2M + H] $^+$  1178.5.  $^1\text{H}$ -NMR  $\delta_{\text{H}}$  (acetone-d<sub>6</sub>, 500 MHz): 3.34 (m, 1H, NHCH<sub>2</sub>CH<sub>2</sub>), 3.52 (m, 1H, NHCH<sub>2</sub>CH<sub>2</sub>), 3.58 (m, 1H, CH<sub>2</sub>CH<sub>2</sub>N), 3.73 (m, 1H, CH<sub>2</sub>CH<sub>2</sub>N), 4.19 (m, 1H, FMOC-CHCH<sub>2</sub>), 4.25 (s, 2H, NCH<sub>2</sub>COOH), 4.33–4.39 (dd, 2H, CHCH<sub>2</sub>O), 6.60 (bs, 1H, NH), 7.30–7.33 (t, 2H, FMOC), 7.39–7.42 (t, 2H, FMOC), 7.60–7.66 (m, 3H, Ph), 7.70–7.72 (m, 4H, FMOC + Ph), 7.86–7.88 (d, 2H, FMOC), 8.20–8.23 (m, 4H, Ph).  $^{13}\text{C}$ -NMR (acetone-d<sub>6</sub>, 126 MHz): 41.31, 47.42, 48.00, 50.53, 67.13, 120.78, 126.08, 127.63, 127.74, 127.94, 128.31, 128.54, 128.69, 130.90, 130.94, 137.78, 139.60, 142.15, 145.17, 156.98, 165.37, 171.28, 171.81. HR ESI-MS calc for C<sub>33</sub>H<sub>29</sub>N<sub>6</sub>O<sub>5</sub> [M + H] $^+$  589.2194, found 589.2196.

**NLS-Pra, NLS-tetra and PNA.** The peptides and the PNA sequences were synthesized by solid phase synthesis, as previously reported by our group on a TENTA Gel-S-RAM resin.<sup>28,53</sup> All the amine groups in peptide and PNA sequences are present as TFA salts. **NLS-Pra:** ESI-MS (pos. detection mode):  $m/z$  [M + H] $^+$  931.6, [M + 2H] $^{2+}$  466.4, [M + 3H] $^{3+}$  311.4. UPLC r.t. (2.5 min): 0.8 min. **NLS-tetra:** ESI-MS (pos. detection mode):  $m/z$  [M + H] $^+$  962.7, [M + 2H] $^{2+}$  481.9, [M + 3H] $^{3+}$  321.7. UPLC r.t. (2.5 min): 0.7 min. **PNA:** ESI-MS (pos. detection



mode):  $m/z$  [M + 6H]<sup>6+</sup> 865.2, [M + 7H]<sup>7+</sup> 741.8, [M + 8H]<sup>8+</sup> 649.2, [M + 9H]<sup>9+</sup> 577.1. UPLC r.t. (2.5 min): 0.9 min.

**Mn-maleimide 4A.** **A** as trifluoroacetate salt (30 mg, 0.067 mmol, 1.0 eq.) and maleic anhydride (66 mg, 0.67 mmol, 10.0 eq.) were dissolved in glacial acetic acid (1 mL) and then refluxed for 8 h. The solvent was then evaporated using a high vacuum pump. The crude product was then purified by column chromatography on silica gel with DCM : MeOH (100 : 2.5) as the eluent. The product was isolated as the first band (r.f. 0.67). The solvent was removed using a rotary evaporator to yield 16.6 mg of the expected product as a light brown oil (60%). <sup>1</sup>H-NMR  $\delta$ <sub>H</sub> (CDCl<sub>3</sub>, 500 MHz): 1.79 (m, 2H, CH<sub>2</sub>CH<sub>2</sub>CH<sub>2</sub>), 2.18 (t, 2H, CpCH<sub>2</sub>CH<sub>2</sub>), 2.26 (t, 2H, CH<sub>2</sub>CH<sub>2</sub>CO), 3.45–3.47 (m, 2H, NHCH<sub>2</sub>CH<sub>2</sub>), 3.69–3.70 (m, 2H, CH<sub>2</sub>CH<sub>2</sub>NH), 4.63 (s, 4H, Cp), 5.81 (br s, 1H, NH), 6.73 (s, 2H, maleimide). <sup>13</sup>C-NMR (CDCl<sub>3</sub>, 126 MHz): 26.68, 27.74, 35.85, 37.76, 39.17, 81.96, 106.32, 134.43, 171.10, 172.62, 225.33. ESI-MS (pos. detection mode):  $m/z$  [M + H<sup>+</sup>] 413.1. UPLC r.t. (2.5 min): 1.3 min.

**Fc-maleimide 4B.** **B** (30 mg, 0.140 mmol, 1.0 eq.) and maleic anhydride (137 mg, 1.40 mmol, 10.0 eq.) were dissolved in glacial acetic acid (1 mL) and then refluxed for 6 h. The solvent was then evaporated using a high vacuum pump. The crude product was then purified by column chromatography on silica gel with DCM as the eluent. The product was isolated as the first orange band (r.f. 0.75). The solvent was removed using a rotary evaporator to yield 1.8 mg of product (4%). <sup>1</sup>H-NMR  $\delta$ <sub>H</sub> (CDCl<sub>3</sub>, 500 MHz): 4.10 (m, 2H, Cp), 4.17 (s, 5H, Cp), 4.28 (m, 2H, Cp), 4.44 (s, 2H, CH<sub>2</sub>), 6.64 (s, 2H, maleimide). <sup>13</sup>C-NMR (CDCl<sub>3</sub>, 126 MHz): 37.20, 68.47, 68.78, 69.54, 134.18, 170.48. ESI-MS (pos. detection mode):  $m/z$  [M]<sup>+</sup> 295.0. UPLC r.t. (2.5 min): 1.6 min.

**2A. A** (20 mg, 0.045 mmol, 1.0 eq.) in 30  $\mu$ L of MeOH, CuSO<sub>4</sub> (0.143 mg, 0.0009 mmol, 0.02 eq.) in 15  $\mu$ L of H<sub>2</sub>O and NaHCO<sub>3</sub> (7.6 mg, 0.089 mmol, 2.0 eq.) in 200  $\mu$ L of H<sub>2</sub>O were mixed in a 10 mL round bottom flask. TfN<sub>3</sub> (0.134 mmol, 3.0 eq.), freshly prepared as previously reported,<sup>22</sup> in 124  $\mu$ L of DCM was then added to this mixture. 1.6 mL of MeOH were added to the solution to make it homogeneous. The mixture was then stirred for 30 min until both TLC (Hex : EtOAc 1 : 1) and UPLC (r.t. 1.35 min,  $m/z$  = 359.1) confirmed the full conversion of the amine group to the azide. The mixture was then transferred in a microwave reactor and the following reagents were added to it: Fmoc-L-Pra-OH (15.1 mg, 0.045 mmol, 1.0 eq.), TBTA (2.4 mg, 0.0045 mmol, 0.1 eq.) in 254  $\mu$ L of MeOH, CuSO<sub>4</sub> (0.143 mg, 0.0009 mmol, 0.02 eq.) in 15  $\mu$ L of H<sub>2</sub>O and Na ascorbate (1.78 mg, 0.009 mmol, 0.2 eq.) in 154  $\mu$ L of H<sub>2</sub>O and 0.5 mL of MeOH to help full dissolution. The mixture was refluxed in the MW oven for 1 h at 80 °C (60 W). The solvent was removed at the rotary evaporator and the mixture was purified by column chromatography on silica gel with DCM : MeOH (10 : 1) as the eluent to isolate the product (r.f. 0.27, 50%). Another batch was purified by preparative r.p. HPLC (linear gradient of A (double distilled water containing 0.1% v/v trifluoroacetic acid) and B (acetonitrile):  $t$  = 0–3 min 25% B,  $t$  = 33 min 100% B,  $t$  = 35 min 100% B, flow rate 20 mL min<sup>-1</sup>, detection 275 nm) to afford the same product. ESI-MS (neg. detection mode):  $m/z$  [M – H]<sup>-</sup> 575.1, [2M – H]<sup>-</sup> 1151.3. UPLC r.t. (2.5 min): 1.55 min. HR ESI-MS calc for C<sub>31</sub>H<sub>27</sub>FeN<sub>4</sub>O<sub>4</sub> [M – H]<sup>-</sup> 575.1387, found 575.1391.

**2B. B** (20 mg, 0.093 mmol, 1 eq.) in 158  $\mu$ L of MeOH, CuSO<sub>4</sub> (0.297 mg, 0.00186 mmol, 0.02 eq.) in 30  $\mu$ L of H<sub>2</sub>O and NaHCO<sub>3</sub> (15.7 mg, 0.186 mmol, 2 eq.) in 424  $\mu$ L of H<sub>2</sub>O were mixed in a 10 mL round bottom flask. TfN<sub>3</sub> (0.279 mmol, 3 eq.), freshly prepared as previously reported,<sup>22</sup> in 258  $\mu$ L of DCM was added to the mixture. 2.5 mL of MeOH were added to the solution to make it homogeneous. The mixture was stirred for 1 h, until when both TLC (Hex : EtOAc 1 : 1) and UPLC (r.t. 1.60 min,  $m/z$  = 240.9) confirmed the full conversion of the amine group to azide. Then the mixture was transferred in a microwave reactor and the following reagents were added to it: Fmoc-L-Pra-OH (31.2 mg, 0.093 mmol, 1 eq.), TBTA (4.9 mg, 0.0093 mmol, 0.1 eq.) in 526  $\mu$ L of MeOH, CuSO<sub>4</sub> (0.297 mg, 0.00186 mmol, 0.02 eq.) in 30  $\mu$ L of H<sub>2</sub>O and Na ascorbate (3.68 mg, 0.0186 mmol, 0.2 eq.) in 380  $\mu$ L of H<sub>2</sub>O and 0.5 mL of MeOH to help full dissolution. The mixture was refluxed in MW oven for 1 h at 80 °C (60 W). After the reaction time, the solvent was removed using a rotary evaporator and the mixture was purified by column chromatography on silica gel with DCM : MeOH (10 : 1) as the eluent, to isolate the product (r.f. 0.52, 29%). Another batch was purified by preparative r.p. HPLC (linear gradient of A (double distilled water containing 0.1% v/v trifluoroacetic acid) and B (acetonitrile):  $t$  = 0–3 min 25% B,  $t$  = 33 min 100% B,  $t$  = 35 min 100% B, flow rate 20 mL min<sup>-1</sup>, detection 275 nm) to afford the same compound. ESI-MS (neg. detection mode):  $m/z$  [M – H]<sup>-</sup> 575.1, [2M – H]<sup>-</sup> 1151.3. UPLC r.t. (2.5 min): 1.55 min. HR ESI-MS calc for C<sub>31</sub>H<sub>27</sub>FeN<sub>4</sub>O<sub>4</sub> [M – H]<sup>-</sup> 575.1387, found 575.1391.

**1H-NMR**  $\delta$ <sub>H</sub> (MeOH-d4, 500 MHz): 3.04–3.09 (m, 1H, triazCH<sub>2</sub>CH), 3.33 (below MeOH, m, 1H, triazCH<sub>2</sub>CH), 4.14–4.26 (m, 12H, Fc, OCH<sub>2</sub>CH, CH<sub>2</sub>CHFmoc), 4.49–4.51 (m, 1H, NHCHCOOH), 7.32–7.35 (m, 2H, Fmoc), 7.42–7.45 (m, 2H, Fmoc), 7.62–7.67 (m, 2H, Fmoc), 7.77 (bs, 1H, triaz), 7.85–7.87 (m, 2H, Fmoc). <sup>13</sup>C-NMR (MeOH-d4, 126 MHz): 28.85, 48.27, 51.09, 55.13, 68.26, 121.16, 121.19, 124.25, 126.60, 126.61, 128.43, 129.03, 129.05, 142.67, 142.72, 144.70, 145.33, 145.37, 158.59, 174.59 (Fc signals below MeOH).

**3A. A** (10 mg, 0.0224 mmol, 1.0 eq.) in 254  $\mu$ L of MeOH, CuSO<sub>4</sub> (0.071 mg, 0.00045 mmol, 0.02 eq.) in 11  $\mu$ L of H<sub>2</sub>O and NaHCO<sub>3</sub> (3.8 mg, 0.0448 mmol, 2.0 eq.) in 100  $\mu$ L of H<sub>2</sub>O were mixed in a 10 mL round bottom flask. Then TfN<sub>3</sub> (0.067 mmol, 3.0 eq.), freshly prepared as previously reported, in 34  $\mu$ L of DCM was added to the mixture. 500  $\mu$ L of MeOH were added to the mixture to make it homogeneous. The mixture was stirred for 30 min, until when both TLC (Hex : EtOAc 1 : 1) and UPLC (r.t. 1.35 min,  $m/z$  = 359.1) confirmed the full conversion of the amine group to azide. Then the mixture was transferred in a microwave reactor and the following reagents were added



to it: **NLS-Pra** as TFA salt (31.07 mg, 0.0224 mmol, 1 eq.) in 2.24 mL of H<sub>2</sub>O, TBTA (1.19 mg, 0.00224 mmol, 0.1 eq.) in 474  $\mu$ L of MeOH, CuSO<sub>4</sub> (0.071 mg, 0.00045 mmol, 0.02 eq.) in 11  $\mu$ L of H<sub>2</sub>O and Na ascorbate (0.888 mg, 0.00448 mmol, 0.2 eq.) in 81  $\mu$ L of H<sub>2</sub>O and 2.5 mL of MeOH to help full dissolution. The mixture was refluxed in MW oven for 1 h at 80 °C (60 W). After the reaction time, the solvent was removed using a rotary evaporator and the crude was purified by preparative r.p. HPLC (linear gradient of A (double distilled water containing 0.1% v/v trifluoroacetic acid) and B (acetonitrile):  $t = 0$ –1.48 min 5% B,  $t = 38$  min 100% B,  $t = 40$  min 100% B, flow rate 20 mL min<sup>-1</sup>, detection 275 nm). Chromatographic yield: 65%. ESI-MS (pos. detection mode):  $m/z$  [M + H]<sup>+</sup> 1289.6, [M + 2H]<sup>2+</sup> 645.8, [M + 3H]<sup>3+</sup> 430.7. UPLC r.t. (2.5 min): 0.9 min. MALDI-TOF [M – Mn(CO)<sub>3</sub> + H]<sup>+</sup> 1151.7, [M – Mn(CO)<sub>3</sub> + Na]<sup>+</sup> 1173.7, [M – Mn(CO)<sub>3</sub> + K]<sup>+</sup> 1189.6, [M + H]<sup>+</sup> 1289.6.

**3B. B** (2.73 mg, 0.0127 mmol, 1.0 eq.) in 57  $\mu$ L of MeOH, CuSO<sub>4</sub> (0.04 mg, 0.00025 mmol, 0.02 eq.) in 4  $\mu$ L of H<sub>2</sub>O and NaHCO<sub>3</sub> (2.14 mg, 0.025 mmol, 2.0 eq.) in 57  $\mu$ L of H<sub>2</sub>O were mixed in a 10 mL round bottom flask. Then TfN<sub>3</sub> (0.038 mmol, 3 eq.), freshly prepared as previously reported, in 35  $\mu$ L of DCM was added to the mixture. 400  $\mu$ L of MeOH were added to the solution to make it homogeneous. The mixture was stirred for 1 h, until when both TLC (Hex:EtOAc 1:1) and UPLC (r.t. 1.35 min,  $m/z$  = 240.9) confirmed the full conversion of the amine group to the azide. Then the mixture was transferred in a microwave reactor and the following reagents were added to it: **NLS-Pra** as TFA salt (17.6 mg, 0.0127 mmol, 1 eq.) in 760  $\mu$ L of H<sub>2</sub>O, TBTA (0.672 mg, 0.00126 mmol, 0.1 eq.) in 71  $\mu$ L of MeOH, CuSO<sub>4</sub> (0.04 mg, 0.00025 mmol, 0.02 eq.) in 4  $\mu$ L of H<sub>2</sub>O and Na ascorbate (0.50 mg, 0.00254 mmol, 0.2 eq.) in 44  $\mu$ L of H<sub>2</sub>O and 1 mL of MeOH to help full dissolution. The mixture was refluxed in MW oven for 1 h at 80 °C (60 W). After the reaction time, the solvent was removed using a rotary evaporator and the crude was purified by preparative r.p. HPLC (linear gradient of A (double distilled water containing 0.1% v/v trifluoroacetic acid) and B (acetonitrile):  $t = 0$ –1.48 min 5% B,  $t = 38$  min 100% B,  $t = 40$  min 100% B, flow rate 20 mL min<sup>-1</sup>, detection 275 nm method). Chromatographic yield: 6.5%. ESI-MS (pos. detection mode):  $m/z$  [M – Fc – CH<sub>2</sub> + 3H]<sup>3+</sup> 325.7, [M + 3H]<sup>3+</sup> 391.7, [M – Fc – CH<sub>2</sub> + 2H]<sup>2+</sup> 487.9, [M + 2H]<sup>2+</sup> 586.9, [M + H]<sup>+</sup> 1172.6. UPLC r.t. (2.5 min): 0.9 min. MALDI-TOF [M + H]<sup>+</sup> 1172.6.

**5A. 4A** (4.48 mg, 0.011 mmol, 1 eq.) and **9** (7 mg, 0.011 mmol, 1 eq.) were dissolved in 3 mL CH<sub>3</sub>CN in a fluorescence quartz cuvette and irradiated at 302 nm for 1 h. The mixture turned yellow during irradiation. The solvent was removed at rotatory evaporator and the crude was purified by preparative r.p. HPLC (linear gradient of A (double distilled water containing 0.1% v/v trifluoroacetic acid) and B (acetonitrile):  $t = 0$ –3 min 25% B,  $t = 33$  min 100% B,  $t = 35$  min 100% B, flow rate 20 mL min<sup>-1</sup>, detection 275 nm), to isolate **5A** (chromatographic yield: 8.5%) and the byproduct without the fragment Mn(CO<sub>3</sub>) (chromatographic yield: 40%). ESI-MS (pos. detection mode):  $m/z$  [M + H]<sup>+</sup> 1029.4, [M + H – tBu]<sup>+</sup> 973.3. UPLC r.t. (2.5 min): 1.8 min.

**5B. 4B** (1.2 mg, 0.004 mmol, 1 eq.) and **9** (2.63 mg, 0.004 mmol, 1 eq.) were dissolved in 0.6 mL CH<sub>3</sub>CN in a fluorescence quartz cuvette and irradiated at 302 nm for 1 h. The mixture turned yellow during irradiation. The solvent was dried at rotatory evaporator and the crude was purified by column chromatography on silica gel with eluent DCM:MeOH (10:1). The yellow spot was isolated (r.f. 0.3) to yield the product and a yellow/green solid (2.3 mg, 63%). <sup>1</sup>H-NMR not meaningful due to traces of paramagnetic impurities. <sup>13</sup>C-NMR (CDCl<sub>3</sub>, 126 MHz): 28.27, 29.41, 29.83, 39.41, 47.37, 65.98, 67.18, 114.74, 120.18, 121.97, 125.39, 127.36, 127.93, 129.34, 132.07, 136.33, 141.47, 144.16, 169.30. Some quaternary signals not observed. ESI-MS (pos. detection mode):  $m/z$  [M]<sup>+</sup> 911.4. HR ESI-MS calc for C<sub>52</sub>H<sub>50</sub>FeN<sub>5</sub>O<sub>7</sub> [M + H]<sup>+</sup> 912.3054, found 912.3041. UPLC r.t. (2.5 min): 1.8 min.

**6B. 4B** (0.191 mg, 0.00065 mmol, 1 eq.) and **NLS-tetra** as TFA salt (1 mg, 0.00065 mmol, 1 eq.) were dissolved in 1 mL of DMSO and irradiated in a luminescence quartz cuvette for 1 h. The mixture was purified by preparative r.p. HPLC (linear gradient of A (double distilled water containing 0.1% v/v trifluoroacetic acid) and B (acetonitrile):  $t = 0$ –1.48 min 5% B,  $t = 38$  min 100% B,  $t = 40$  min 100% B, flow rate 20 mL min<sup>-1</sup>, detection 275 nm). Chromatographic yield: 20%. ESI-MS (pos. detection mode):  $m/z$  [M + 4H]<sup>4+</sup> 308.3, [M + 3H]<sup>3+</sup> 410.7, [M + 2H]<sup>2+</sup> 615.4. UPLC r.t. (2.5 min): 0.9 min. MALDI-TOF [M + H]<sup>+</sup> 1229.6.

**Fc-PNA 11. 4B** (0.54 mg, 0.00184 mmol, 5 eq.) and **PNA** as TFA salt (2.5 mg, 0.00037 mmol, 1 eq.) were dissolved in 1 mL of H<sub>2</sub>O in a quartz luminescence cuvette and irradiated for 1 h. The components of the mixture were isolated by preparative r.p. HPLC (linear gradient of A (double distilled water containing 0.1% v/v trifluoroacetic acid) and B (acetonitrile):  $t = 0$ –1.48 min 5% B,  $t = 38$  min 100% B,  $t = 40$  min 100% B, flow rate 20 mL min<sup>-1</sup>, detection 275 nm). **11**: 10%, ESI-MS (pos. detection mode):  $m/z$  [M + 6H]<sup>6+</sup> 909.7, [M + 7H]<sup>7+</sup> 780.0, [M + 8H]<sup>8+</sup> 682.6, [M + 9H]<sup>9+</sup> 606.8. UPLC r.t. (2.5 min): 0.7 min. MALDI-TOF:  $m/z$  5448.2 [M]<sup>+</sup>. **12**: 2.6%, ESI-MS (pos. detection mode):  $m/z$  [M + 6H]<sup>6+</sup> 959.0, [M + 7H]<sup>7+</sup> 822.1, [M + 8H]<sup>8+</sup> 719.5, [M + 9H]<sup>9+</sup> 639.7, [M + 10H]<sup>10+</sup> 575.7. UPLC r.t. (2.5 min): 1.0 min. MALDI-TOF:  $m/z$  5744.9 [M]<sup>+</sup>. **13**: 36%, ESI-MS (pos. detection mode):  $m/z$  [M + 5H]<sup>5+</sup> 1094.8, [M + 6H]<sup>6+</sup> 912.7, [M + 7H]<sup>7+</sup> 782.5, [M + 8H]<sup>8+</sup> 684.8. UPLC r.t. (2.5 min): 0.8 min. MALDI-TOF:  $m/z$  5466.8 [M]<sup>+</sup>. **14**: 17%, ESI-MS (pos. detection mode):  $m/z$  [M + 5H]<sup>5+</sup> 1035.8, [M + 6H]<sup>6+</sup> 863.6, [M + 7H]<sup>7+</sup> 740.3, [M + 8H]<sup>8+</sup> 648.1. UPLC r.t. (2.5 min): 0.7 min.

## Conclusions

The functionalization of biologically relevant molecules with metal complexes is a very intriguing topic nowadays. The insertion of a metal fragment can strongly improve the properties of the system, from a therapeutic or diagnostic point of view as well as for the investigation of biological mechanisms. The use of copper-catalyzed azide–alkyne cycloaddition is deeply



exploited for the functionalization of biomolecules, but some drawbacks limit its application for example *in vivo*. Therefore, the optimization of modified click procedure was extensively studied in the recent years. In this paper we present the use of modified click strategies (namely *one-pot click* and *photoclick*) to insert organometallic fragments in peptides and PNA sequences. *One-pot click* allows for the *in situ* conversion of an amine to the azide intermediate, which is then directly *clicked* with the alkynyl counterpart. Therefore, the isolation of the azide containing compound is not required, relieving the safety concerns linked to the manipulation of azide compounds. We obtained high labelling efficiencies using *one-pot click* on an amine derivative of cymantrene for derivatization of both a model alkynyl amino acid and a NLS peptide carrying this amino acid. When a ferrocene derivative was used as an amine substrate, yields were found to be lower. The harsh conditions used for *one-pot click* (1 h of microwave assisted reflux at 80 °C) might lead to the decomposition of the methylaminoferrocene precursor. We also investigated the application of metal-free *photoclick* to our metal-containing precursors, to establish a biocompatible strategy for organometallic derivatization of biomolecules. While the use of cymantrene as substrate for *photoclick* yielded mainly a by product of the light-mediated CO release from the metal core, the application of *photoclick* to a ferrocene-maleimide derivative allowed for fast and effective functionalization of both a tetrazole-derivatized PNA monomer and a NLS peptide containing this PNA residue. This technique was also used for Fc insertion into a 15-mer PNA sequence carrying the tetrazole group, with yields comparable to those of a previously reported *photoclick* application for dsDNA functionalization.<sup>39</sup> Overall, we envisage the application of these very versatile techniques for the functionalization of biomolecules with other metal complexes. As a result, a wide range of metal fragments could be introduced into bioactive systems to prepare novel diagnostic tools useful to study cellular mechanisms. One could also imagine that novel therapeutic entities could be designed, for example, with the introduction of ruthenium complexes into targeting peptides to obtain selective compounds for traditional chemotherapy or photodynamic therapy. Overall, this study will expand the pool of metal-based probe-containing systems, which can be profitably applied in chemical biology or in medicinal chemistry.

## Acknowledgements

This work was financially supported by the Swiss National Science Foundation (Ambizione Fellowship No. PZ00P2\_126404 as well as Professorships No. PP00P2\_133568 and PP00P2\_157545 to G.G), the University of Zurich (G.G), the Stiftung für wissenschaftliche Forschung of the University of Zurich (G.G.) and the Forschungskredit of the University of Zurich (Grant K-73532-01-01 to C.M). The authors thank Dr Thomas Fox for his help with the NMR experiments and Dr Phuc Ung for helpful discussions.

## References

- 1 R. Mahato, W. Tai and K. Cheng, *Adv. Drug Delivery Rev.*, 2011, **63**, 659–670.
- 2 T. J. S. Binghe Wang and R. A. Soltero, *Drug Delivery: Principles and Applications*, John Wiley & Sons, Inc., Hoboken, 2005.
- 3 V. Stella, R. Borchardt, M. Hageman, R. Oliyai, H. Maag and J. Tilley, *Prodrugs: Challenges and Rewards*, Springer, New York, 2007.
- 4 G. Gasser, *Inorganic Chemical Biology*, Wiley-VCH Verlag GmbH & Co. KGaA, UK, 2014.
- 5 C. Preusch Peter, in *Medicinal Inorganic Chemistry*, American Chemical Society, 2005, vol. 903, pp. 15–29.
- 6 C. Mari, V. Pierroz, A. Leonidova, S. Ferrari and G. Gasser, *Eur. J. Inorg. Chem.*, 2015, **2015**, 3879–3891.
- 7 A. Leonidova, P. Anstaett, V. Pierroz, C. Mari, B. Spingler, S. Ferrari and G. Gasser, *Inorg. Chem.*, 2015, **54**, 9740–9748.
- 8 A. Leonidova, C. Foerster, K. Zarschler, M. Schubert, H.-J. Pietzsch, J. Steinbach, R. Bergmann, N. Metzler-Nolte, H. Stephan and G. Gasser, *Chem. Sci.*, 2015, **6**, 5601–5616.
- 9 S. Jaracz, J. Chen, L. V. Kuznetsova and I. Ojima, *Bioorg. Med. Chem.*, 2005, **13**, 5043–5054.
- 10 J. S. Butler and P. J. Sadler, *Curr. Opin. Chem. Biol.*, 2013, **17**, 175–188.
- 11 V. Fernandez-Moreira, F. L. Thorp-Greenwood and M. P. Coogan, *Chem. Commun.*, 2010, **46**, 186–202.
- 12 M. Meldal and C. W. Tornøe, *Chem. Rev.*, 2008, **108**, 2952–3015.
- 13 M. D. Best, *Biochemistry*, 2009, **48**, 6571–6584.
- 14 W. Tang and M. L. Becker, *Chem. Soc. Rev.*, 2014, **43**, 7013–7039.
- 15 G. Gasser, in *Peptide Nucleic Acids*, ed. P. E. Nielsen and D. H. Appella, Humana Press, 2013, vol. 1050, pp. 55–72.
- 16 G. Gasser, A. M. Sosniak and N. Metzler-Nolte, *Dalton Trans.*, 2011, **40**, 7061–7076.
- 17 A. Leonidova, V. Pierroz, L. A. Adams, N. Barlow, S. Ferrari, B. Graham and G. Gasser, *ACS Med. Chem. Lett.*, 2014, **5**, 809–814.
- 18 S. Bräse, C. Gil, K. Knepper and V. Zimmermann, *Angew. Chem., Int. Ed.*, 2005, **44**, 5188–5240.
- 19 P. Ostrovskis, C. M. R. Volla, M. Turks and D. Markovic, *Curr. Org. Chem.*, 2013, **17**, 610–640.
- 20 C. P. Ramil and Q. Lin, *Curr. Opin. Chem. Biol.*, 2014, **21**, 89–95.
- 21 M. A. Tasdelen and Y. Yagci, *Angew. Chem., Int. Ed.*, 2013, **52**, 5930–5938.
- 22 H. S. G. Beckmann and V. Wittmann, *Org. Lett.*, 2007, **9**, 1–4.
- 23 Y. Wang, C. I. Rivera Vera and Q. Lin, *Org. Lett.*, 2007, **9**, 4155–4158.
- 24 M. Patra, G. Gasser, M. Wenzel, K. Merz, J. E. Bandow and N. Metzler-Nolte, *Organometallics*, 2012, **31**, 5760–5771.
- 25 P. D. Beer and D. K. Smith, *Dalton Trans.*, 1998, 417–424.
- 26 A. Vessières, M. Salmain, P. Brossier and G. Jaouen, *J. Pharm. Biomed. Anal.*, 1999, **21**, 625–633.

27 M. Salmain, A. Vessières, P. Brossier, I. S. Butler and G. Jaouen, *J. Immunol. Methods*, 1992, **148**, 65–75.

28 A. Leonidova, V. Pierroz, R. Rubbiani, J. Heier, S. Ferrari and G. Gasser, *Dalton Trans.*, 2014, **43**, 4287–4294.

29 A. Leonidova, V. Pierroz, R. Rubbiani, Y. Lan, A. G. Schmitz, A. Kaech, R. K. O. Sigel, S. Ferrari and G. Gasser, *Chem. Sci.*, 2014, **5**, 4044–4056.

30 W. Hu, K. Splith, I. Neundorf, K. Merz and U. Schatzschneider, *J. Biol. Inorg. Chem.*, 2012, **17**, 175–185.

31 G. Gasser, A. J. Fischmann, C. M. Forsyth and L. Spiccia, *J. Organomet. Chem.*, 2007, **692**, 3835–3840.

32 R. Jiang, Y. Zhang, Y.-C. Shen, X. Zhu, X.-P. Xu and S.-J. Ji, *Tetrahedron*, 2010, **66**, 4073–4078.

33 R. K. V. Lim and Q. Lin, *Acc. Chem. Res.*, 2011, **44**, 828–839.

34 W. Song, Y. Wang, J. Qu, M. M. Madden and Q. Lin, *Angew. Chem., Int. Ed.*, 2008, **47**, 2832–2835.

35 Y. Wang, W. Song, W. J. Hu and Q. Lin, *Angew. Chem., Int. Ed.*, 2009, **48**, 5330–5333.

36 W. Song, Y. Wang, J. Qu, M. M. Madden and Q. Lin, *Angew. Chem., Int. Ed.*, 2008, **47**, 2832–2835.

37 G. Gasser, N. Huesken, S. D. Koster and N. Metzler-Nolte, *Chem. Commun.*, 2008, 3675–3677.

38 G. Dordelmann, T. Meinhardt, T. Sowik, A. Krueger and U. Schatzschneider, *Chem. Commun.*, 2012, **48**, 11528–11530.

39 S. Arndt and H.-A. Wagenknecht, *Angew. Chem., Int. Ed.*, 2014, **53**, 14580–14582.

40 P. E. Nielsen, M. Egholm, R. H. Berg and O. Buchardt, *Science*, 1991, **254**, 1497–1500.

41 P. Anstaett, Y. Zheng, T. Thai, A. M. Funston, U. Bach and G. Gasser, *Angew. Chem., Int. Ed.*, 2013, **52**, 4217–4220.

42 P. Anstaett and G. Gasser, *Chimia*, 2014, **68**, 264–268.

43 P. E. Nielsen, *Curr. Opin. Mol. Ther.*, 2000, **2**, 282–287.

44 C. Mari, M. Panigati, L. D'Alfonso, I. Zanoni, D. Donghi, L. Sironi, M. Collini, S. Maiorana, C. Baldoli, G. D'Alfonso and E. Licandro, *Organometallics*, 2012, **31**, 5918–5928.

45 T. Joshi, M. Patra, L. Spiccia and G. Gasser, *Artif. DNA PNA XNA*, 2013, **4**, 11–18.

46 G. Gasser, A. Pinto, S. Neumann, A. M. Sosniak, M. Seitz, K. Merz, R. Heumann and N. Metzler-Nolte, *Dalton Trans.*, 2012, **41**, 2304–2313.

47 G. Gasser, A. M. Sosniak, A. Leonidova, H. Braband and N. Metzler-Nolte, *Aust. J. Chem.*, 2011, **64**, 265–272.

48 G. Gasser, K. Jaeger, M. Zenker, R. Bergmann, J. Steinbach, H. Stephan and N. Metzler-Nolte, *J. Inorg. Biochem.*, 2010, **104**, 1133–1140.

49 Z. Ma, F. Olechnowicz, Y. A. Skorik and C. Achim, *Inorg. Chem.*, 2011, **50**, 6083–6092.

50 D.-L. Popescu, T. J. Parolin and C. Achim, *J. Am. Chem. Soc.*, 2003, **125**, 6354–6355.

51 R. M. Franzini, R. M. Watson, G. K. Patra, R. M. Breece, D. L. Tierney, M. P. Hendrich and C. Achim, *Inorg. Chem.*, 2006, **45**, 9798–9811.

52 M. Robaczewska, R. Narayan, B. Seigneres, O. Schorr, A. Thermet, A. J. Podhajska, C. Trepo, F. Zoulim, P. E. Nielsen and L. Cova, *J. Hepatol.*, 2004, **42**, 180–187.

53 *Peptide Nucleic Acids: Methods and Protocols*, ed. P. E. Nielsen and D. H. Appella, Humana Press, 2014.

